Available online at www.sciencedirect.com
ScienceDirect
Journal of Theoretical Biology 243 (2006) 287–298
Journal of Theoretical Biology
www.elsevier.com/locate/yjtbi

The growth and form of tunnelling networks in ants

Jérôme Buhl[a,*], Jacques Gautrais[a], Jean Louis Deneubourg[b], Pascale Kuntz[c], Guy Theraulaz[a]

[a]Centre de Recherches sur la Cognition Animale, CNRS UMR 5169, Université Paul Sabatier, 118 route de Narbonne, 31062 Toulouse Cedex 4, France
[b]Unit of Social Ecology, CP 231, Université Libre de Bruxelles, Campus Plaine, Boulevard du Triomphe, 1050 Bruxelles, Belgium
[c]Laboratoire d'Informatique Nantes-Atlantique, Université de Nantes, 2 rue de la Houssinière, BP 92208, 44322 Nantes Cedex 03, France

Received 9 September 2005; received in revised form 14 June 2006; accepted 15 June 2006
Available online 29 June 2006

Abstract

Many biological networks grow under strong spatial constraints, where the large-scale structure emerges from the extension, the branching and intersection of growing parts of the network. One example is provided by ant tunnelling networks, which represent the most common nest architecture in ants. Our goal was to understand how these network structures emerge from the tunnel growth dynamics. We used a standardized two-dimensional set-up shaped as a disk and studied the characteristics of tunnel growth in terms of initiation, propagation and termination of new digging sites and found that they can be described with simple probabilistic laws. We show that a model based on these simple laws and for which parameters were measured from the sand disks experiments can account for the emergence of several topological properties that were observed in experimental networks. In particular, the model accurately reproduced an allometric relation between the number of edges and the number of nodes, as well as an invariance of the node degree distribution. The model was then used to make predictions about the resulting networks' topology when the geometry of the sand substrate was shaped as a square. Experiments aimed at testing the model's predictions showed that the predictions were indeed validated. Both in the model and in the experiments, there was a similar trend for the node degree distribution tail to be steeper in the square sand patch than in the disk sand patch, while other characteristics such as the meshedness (i.e. how densely the network is internally connected) remained constant. Because network growth based on branching/fusion events is widespread in biological systems, this general model might provide useful insights for the study of other systems and, more generally, the evolution of spatial networks in biological systems.

Keywords: Network topology; Network growth; Tunnelling networks; Messor sancta

1. Introduction

Many species of ants build their nest by excavation. A typical underground nest structure is composed of a large number of chambers interconnected by a network of galleries (Brian, 1983; Cerdan, 1989; Délye, 1971; Frisch, 1975; Rasse, 1999; Thomé, 1972). Despite the functional importance of these structures, there only exist a few detailed descriptions and quantitative studies of subterranean networks built in natural conditions (Cassill et al., 2002; Mikheyev and Tschinkel, 2004; Tschinkel, 1987, 2004). Excavations and plaster casts of ant nests have revealed that while they are built with the same basic elements, ant nests exhibit species-specific patterns in the way galleries and chambers are organized. In particular, nests show large variations in their branching pattern, whether they are composed of only one vertical shaft connecting one or few chambers (Tschinkel, 2003), several branched shafts (Mikheyev and Tschinkel, 2004) or a mesh-like pattern of interconnected galleries (Cassill et al., 2002). It seems these variations may be correlated with colony size: the greater the number of individuals in a colony, the greater the amount of branching and the complexity of the nest (Cassill et al., 2002).

Structure often affects function. One important question is whether a colony's efficient performance of certain tasks depends on the topological organization of the network structures it inhabits. For example, is there any relationship between the spatial organization of a network of

*Corresponding author. Present address: School of Biological Sciences, Heydon-Laurence building, A08, The University of Sydney, NSW 2006, Australia. Tel.: +61 (0) 2 9036 7225; fax: +61 (0) 2 9351 4119.
E-mail address: jerome.buhl@bio.usyd.edu.au (J. Buhl).

0022-5193/$ - see front matter © 2006 Elsevier Ltd. All rights reserved.
doi:10.1016/j.jtbi.2006.06.018

galleries and its efficiency with regards to the traffic of ants inside the nest or its robustness against disruptions that may occur in the network? Since networks are the result of growth processes, a second major question is to understand which underlying mechanisms may account for the emergence of the network structures.

There is currently little information about tunnel growth, with the exception of studies involving isolated workers. It has been shown that in the presence of moist sand in laboratory conditions, isolated workers from various species readily excavate tunnels using similar behaviours (Sudd, 1969). There exist inter-specific differences as regards several characteristics of the tunnelling patterns built by isolated individuals. Some species, such as *Formica lemani*, exhibit a preference to excavate vertically oriented tunnels while others, such as *Lasius niger*, do not; lateral branching (initiations of new tunnels along an existing tunnel wall) occurs frequently in some species but seldom in others (Sudd, 1970a). Though Sudd never observed how lateral branching is initiated, he showed that isolated workers of *Lasius niger* often dig not only at the front but also on the wall of the tunnels, while workers of *Formica lemani* focused their digging activity nearly exclusively at the front (Sudd, 1970b). Such differences in digging behaviour may partly account for the architectural differences observed in the nests built by these two species. However, as mentioned by Sudd (1975), "further levels might concern the interaction of ants with one another, or the interaction of tunnels to form more complex structures". The former question has been the topic of a few studies that have shown a tendency for an ant to dig at places where other ants have previously dug (Imamura, 1982; Rasse, 1999; Sudd, 1971). Such amplification processes may play an important role in the organization of the collective digging activity (Buhl et al., 2005; Rasse, 1999; Rasse and Deneubourg, 2001). The present paper mainly addresses the latter question. It focuses on the characteristics of tunnel growth and how they can account for the topological properties of the networks at a large scale.

We shall consider the structure of tunnelling networks as a discrete set of interconnected segments of tunnels and will thus describe it by a graph. Graph theory has recently proved to be a powerful tool to characterize complex network topologies in social, economical, biological and technological systems (Albert and Barabasi, 2002; Dorogovtsev and Mendes, 2003; Solé et al., 2002).

We studied the growth of tunnelling networks that are produced by workers of the ant *Messor sancta* in a standardized two-dimensional set-up. In these conditions, the structures are not submitted to strong heterogeneities in the environment and it is possible to quantify the growth dynamics. This set-up enabled us to study under well-controlled laboratory conditions:

(1) The topology of gallery networks by spatial and graph analysis. As we had access to the complete growth history of these networks, the experimental set-up represented a unique opportunity to understand how a particular network topology emerges in the course of growth processes.
(2) The growth characteristics of the tunnels, such as the initiations of new tunnels and their trajectory characteristics (orientation and speed of the tunnel front).

We then developed a model in which the rules of tunnel growth characterizing tunnel initiation, propagation and termination were implemented according to the parameters measured in the experiments. The set of tunnel growth rules used in this model was sufficient to reproduce the topological properties of the networks observed in the experiments. The model was further validated by comparing its predictions to a new set of experiments when using a set-up where sand was shaped as a square rather than as a disk.

2. Materials and methods

2.1. Study species and experimental set-up

We used six colonies of *Messor sancta* collected in South-Western France (Narbonne). All colonies were composed of workers (population range: 2000–5000) and brood. *M. sancta* is a Mediterranean granivorous ant that excavates large nests in sandy grounds. Though never studied in detail, the nest is believed to be structured in two components: a vertical component, connecting superficial to deep chambers by long, non or rarely branched vertical shafts, the deepest chambers reaching several metres depth, and a horizontal component in the form of a large superficial horizontal network of tunnels, sometimes forming a mesh-like pattern, interconnecting several chambers that can be empty, filled with seeds or refuse material (Cerdan, 1989).

The general experimental set-up consisted of a flat layer of sand 5 mm in height that was used as digging substrate. There were two experimental groups: in the first, the sand was shaped as a disk 20 cm in diameter ($N = 19$); in the second, the sand was shaped as a square 17.7 cm in sides ($N = 9$). Hence, the sand area was the same in both groups ($314\,cm^2$).

We used brusselian sand (a yellow sand of a very fine and homogeneous granularity) that was poured in a mould and moistened by spraying water (25 ml). The mould was then removed and the disk sand patch covered by a glass plate (25 cm × 25 cm). To prevent ants from escaping, an arena (diameter 50 cm) with a wall coated with Fluon GP2® was placed around the disk sand patch. Each experiment lasted 3 days and began with the random dispersal of a group of 200 ants around the piece of sand.

The set-up was videotaped from above during the 72 h of experiment in a time-lapse mode at a frequency of 2 s every 20 min with a high-resolution digital camera (SONY DCR-VX1000E) (Fig. 1). Though the initiation of the digging activity on the periphery of the sand patch may

seem somewhat artificial in comparison to the natural conditions in which ant nests are excavated, it represents one of the best solutions to present ants with a homogeneous sand wall that has also a large enough perimeter so that it does not constrains the number of tunnels initiated.

The data were acquired on video frames with image analysis software that allowed the identification of network components. For each sequence in the group of experiments performed with a disk sand patch, we kept 1 frame every 20 min ($N = 217$) to analyse the tunnel growth. In the group of experiments performed with a squared disk, the analysis was performed on the last frame in order to get the topology of the final network.

2.2. Graph topology and spatial analysis

For each frame, we considered the network as an embedded planar graph $G = (V, E)$ (Nishizeki and Chiba, 1988), where V is a set of n nodes characterized by their (x,y) position, label and diameter, and E a set of m edges that link pairs of nodes and characterized by their width and length (Fig. 2).

In the tunnel growth analysis, a label was assigned according to the way the node was constructed. A "*peripheral germ*" corresponds to the initiation of a new tunnel on the periphery of the sand patch. If the new tunnel starts at a position where no other tunnel has been previously built, then a "*peripheral node*" is added to the network structure. "*Lateral germs*" correspond to the initiation of new tunnels inside the sand patch. If a lateral germ does not emerge at the position of an existing node, then a "*lateral node*" is added to the network. From these germs, the emerging new tunnels are characterized by a "*front node*", corresponding to the location of the digging site, and an edge connecting the front node to the node from which it emerged. The edge thus corresponds to the space occupied by the tunnel.

A connected component represents a subset of the graph G, in which there exists at least one path between each pair of nodes of this subset. To determine whether a network was composed of a main connected component or fragmented into several ones, we computed the ratio between the number of nodes in the largest connected component n_l and the total number of nodes n in the network. We will hereafter refer to this ratio as the relative

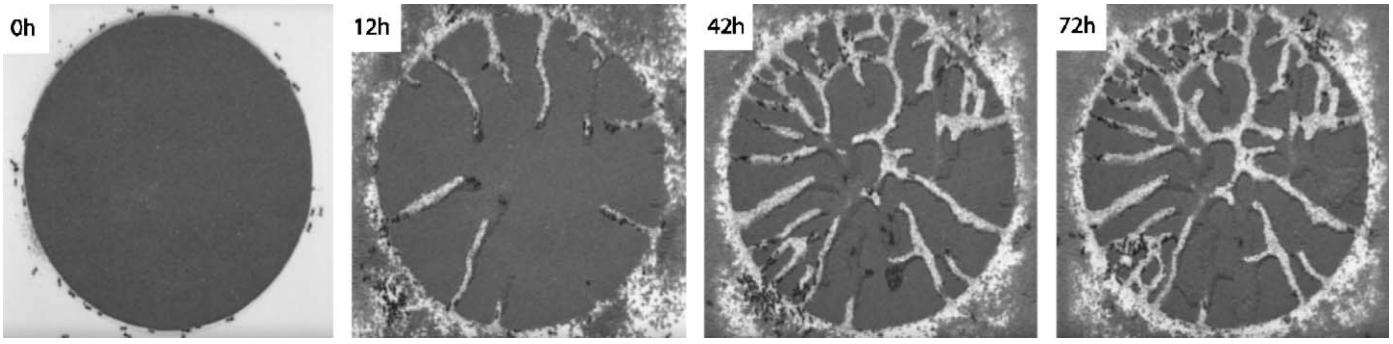

Fig. 1. Example of a gallery pattern produced by 200 ants over 3 days. At the beginning of an experiment, ants are dispersed around the sand patch and can only start to dig from the periphery. After a few hours, several galleries are initiated by groups of workers. These galleries extend inside the sand patch and frequently branch. At the end of the excavation process, after 72 h, the network obtained is the result of the extension, branching and fusing of the tunnels.

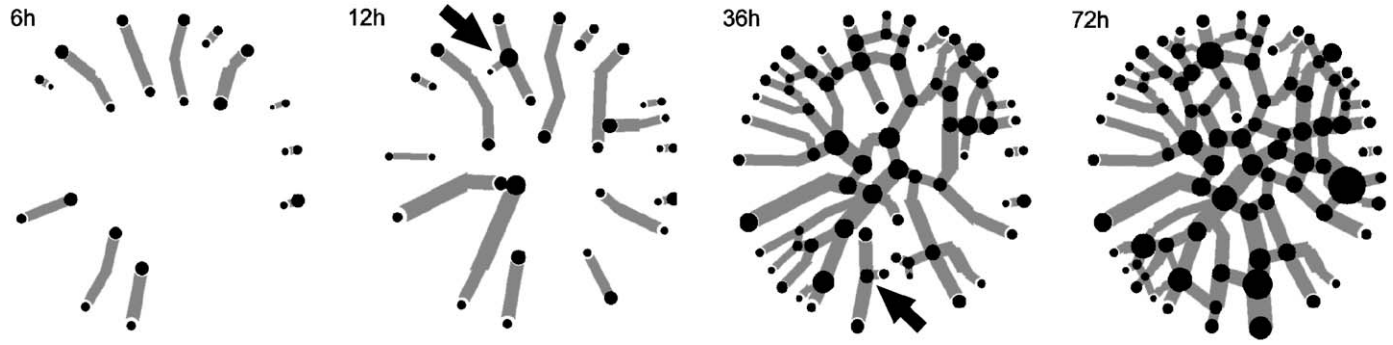

Fig. 2. Example of a graph abstraction produced from the pictures of the same experiment as in Fig. 1. At 6 h, the network is only composed of isolated growing galleries. In the graph, each gallery is represented by a peripheral node at the initiation point of the gallery, and a front node where the gallery is expanding. The two nodes are connected by an edge. At 12 and 36 h, the networks take a more complex form. Some tunnels have already merged with other ones, and lateral branching occurs along existing galleries (two examples are shown with a black arrow). At 72 h, the tunnelling activity has almost stopped, and the network obtained is the result of a complex combination between initiations, branching and intersections of galleries.

size of the largest connected component (V_l/V). For all the following topological measures, the analysis was only performed on the largest connected component.

The allometric relation between the number of edges m and the number of nodes n was estimated by performing a linear regression on the log–log transformation of the data, and the exponent value of the power law was given by the value of the regression coefficient. Note that the relation between m and n is linear when the exponent value is not significantly different from the theoretical value of 1 (see Zar, 1999). The degree k of a node corresponds to the number of edges connected to it. To analyse the node degree distributions, we used the inverse cumulative distribution.

According the Euler formula, the number of internal faces (i.e. regions bounded by the edges, excluding the external face, which corresponds to the infinitely large region extending in the periphery) associated with any planar graph is $f = m - n + 1$. For such graphs $m \leqslant 3n - 6$ and consequently the maximal number of faces is $f_{\max} = 2n - 5$. We can thus compute a normalized "meshedness coefficient" $M = f/f_{\max}$ (Buhl et al., 2004b), where M can vary from zero (tree structure) to one (complete planar graph with all possible edges that do not produce intersections).

All statistical tests were done with SPSS 11.0 for Windows. The T3 Dunnet test was used for post-hoc comparisons with $\alpha = 0.05$. To characterize the log-normal distributions, we use the parameters $\mu^{*\times}/s^*$, corresponding to geometric mean μ^*, and the multiplicative standard deviation s^* (see Limpert et al., 2001).

3. Statistical quantification of the tunnel growth

3.1. Initiation of peripheral germs

In all experiments, we studied the evolution over time of the number of peripheral germs. The number of peripheral germs increased with a maximal rate at the beginning of the experiments and reached a plateau after 3 days. This can be described by the following equation:

$$\frac{dG_p}{dt} = P_g\, G_{\max}\left(1 - \frac{G_p}{G_{\max}}\right), \tag{1}$$

where G_p represents the number of peripheral germs and P_g the probability for a peripheral germ to be initiated. It thus comes that

$$G_p(t)/G_{\max} = 1 - e^{-P_g t}, \tag{2}$$

$G_{\max}$ was estimated by the mean number of peripheral germs observed at the end of the experiments ($G_{\max} = 17.79 \pm 6.6$ SD). We validated this relation on all experiments by performing a linear regression ($R^2 = 0.97$; $P_g = 0.0011\,\mathrm{min}^{-1}$; Fig. 3a) on the linearised form of relation (2). Therefore, we will assume, in our model, the initiation of peripheral germs with a constant probability $P_g = 0.0011\,\mathrm{min}^{-1}$, in the small time approximation.

To study the position of the peripheral germs on the periphery of the sand patch, we analysed the angular distance between the positions of each consecutive peripheral germ. We compared this distribution with the one obtained when 18 peripheral germs (corresponding to the rounded value of $G_{\max}$) were distributed randomly around the sand patch ($N = 50\,000$ simulations). The experimental distribution was similar to the theoretical distribution generated by a random dispersal (Fig. 3b).

3.2. Initiation of lateral germs

In all experiments, we studied the evolution over time of the total length of the network and of the number of lateral germs. We tested the hypothesis that the rate of initiation of lateral germs (G_l) is proportional to the total length L of the network and a constant probability P_l:

$$dG_l/dt = P_l L. \tag{3}$$

To simplify, we will focus on the first 48 h of the experiments, where the length was growing in a linear way:

$$dL/dt = a. \tag{4}$$

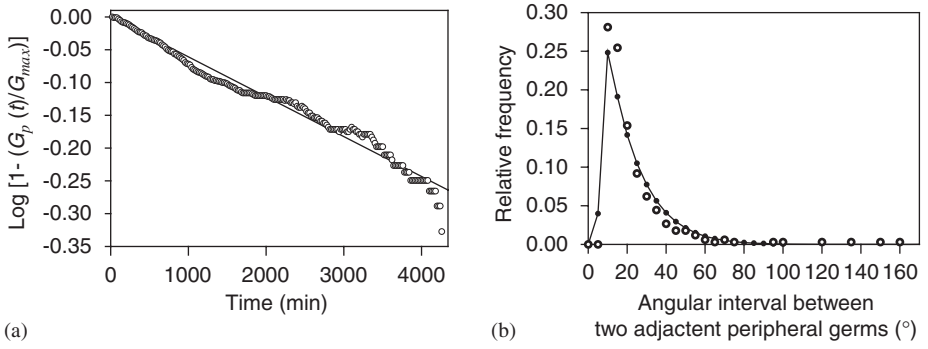

Fig. 3. (a) Regression test performed on the mean dynamics of the cumulative number of peripheral germs following Eq. (2). (b) Distribution of angular intervals between peripheral germs in the experiments (open circles) and in simulations of random dispersal of 18 nodes along the periphery of the sand patch (closed circles and black curve).

The constant $a = 0.56\,\mathrm{mm\,min^{-1}}$ was estimated by a linear regression between the mean total length of tunnels and time during the first 48 h of the experiments ($R^2 = 0.95$). Coupling Eq. (3) and (4), it thus comes that

$$G_l(t) = \frac{P_l}{2a} L^2(t). \quad (5)$$

This relationship (Eq. (5)) was tested in the experiments by a nonlinear regression test for a power law on all pairs ($N = 4123$) of number of lateral germs $G_l(t)$ and total length $L(t)$ ($R^2 = 0.9$; exponent $\lambda = 2.041 \pm 1.53.10^{-3}$ SE; $P_l/2a = 4.693.10^{-4} \pm 3.8.10^{-5}$ SE; see Fig. 4a). Therefore, we will assume that there exists a constant probability per unit of time and network length $P_l = 5.26 \times 10^{-6}\,\mathrm{mm^{-1}\,min^{-1}}$ for a lateral germ to be initiated inside the sand patch.

There were two types of lateral germs: some were initiated along the walls of the tunnels, and thus lead to the formation of new lateral nodes, while some took place at intersections between tunnels, which lead to the emergence of new front nodes connected to the nodes already existing at these intersections. The mean proportion of lateral initiations taking place on an edge was $P_n = 0.689$ (ratio between the mean number of lateral initiations on an edge and the mean total number of lateral initiations, 13.5/19.6).

To study the position of the lateral nodes along an edge (*parent edge*), we analysed the distribution of the relative position of the centre of the lateral nodes between the centres of the two nodes (*parent nodes*) that bounded the parent edge ($N = 200$, we excluded cases in which the new tunnel immediately collided with an existing one). This relative position was computed as the ratio between the distance to the nearest parent node and the sum of the distances to both parent nodes. In addition, we measured the *remaining length* as the sum of the length of the two *daughter* edges (i.e. the edges linking the two parent nodes to the lateral node), but excluding the length covered within the radius of the nodes. Most of the lateral nodes were created on short parent edges, so that their relative position was strongly constrained to be located near the centre of the edges (remaining length <3 cm in 135/200 events). However, when the remaining length was large enough ($\geqslant 3$ cm) to allow more freedom in the location of the germ, it appeared that its relative position was not significantly different from a homogeneous distribution along the parent edge (Kolmogorov–Smirnov test: $N = 65$, $Z = 1.123$, $p = 0.161$; Fig. 4b).

3.3. Initial orientation of the tunnels

In a sample of 10 experiments with the sand patch, we computed the angle formed between the direction of the first 2 cm of the tunnels growing from peripheral germs and the normal vector to the sand patch ($N = 117$ observations). The distribution of orientation of peripheral germs was Gaussian (Fig. 5a) with a mean value $\alpha = -1.3^\circ$ (very close to the normal vector) and a standard deviation $\sigma = 8.44$ (Kolmogorov–Smirnov test, $N = 117$, $Z = 0.697$, $p = 0.716$). Since we could only quantify accurately the orientation of peripheral germs, we will make two assumptions regarding the other types of tunnel initiations: first, we will assume that ants always initiate their tunnel with respect to a sand wall, i.e. in a perpendicular way irrespective of whether the sand wall is on the periphery of the disk or part of an existing tunnel (edge), which is supported by our qualitative observations. In the case of initiations taking place on existing nodes, we did not observe any particular pattern and will assume that they take place randomly around the node.

3.4. Growth speed of the tunnels

To determine the mean growth speed of a tunnel, we measured the average distance over which a front node had moved between two frames. The data was filtered so that only front nodes moving during at least 3 frames were considered ($N = 210$). The distribution was log-normal with a geometric mean value $S^* = 0.062\,\mathrm{mm/min}\,^{\times}/\,1.51$ ($^{\times}/$ indicates the multiplicative standard deviation, as

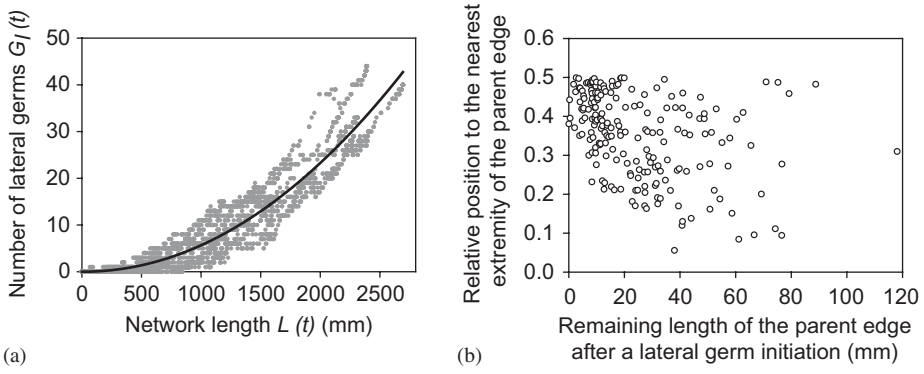

Fig. 4. (a) Experimental and predicted relationship (see Eq. (6)) between the number of lateral germs $G_l(t)$ and the total length of the network $L(t)$ observed at a given time t. (b) Relative position of a lateral node along the parent edge as a function of the remaining length of the gallery at both side the newly created lateral node. Most of lateral nodes appeared around the middle of the parent edge, but with nearly no remaining length of tunnels. When the remaining length of the gallery was long enough to provide a certain degree of freedom in the position of the lateral node (e.g. >30 mm), its relative position appeared to be homogeneously distributed along the parent edge.

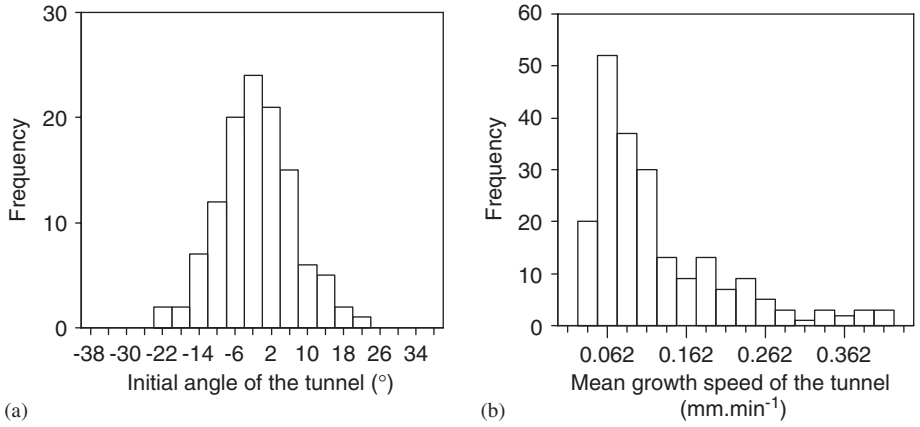

Fig. 5. (a) Distribution of the angles formed between the initial orientation of a new tunnel initiated at the periphery and the normal to the periphery of the sand patch. (b) Distribution of the extension speed of the galleries.

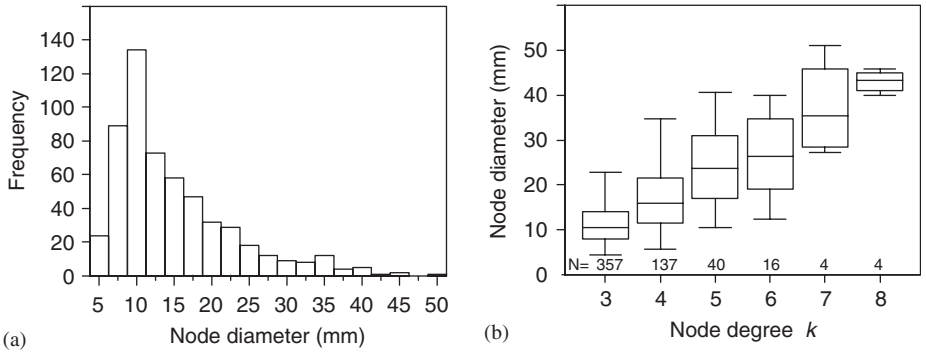

Fig. 6. (a) Distribution of the node diameters. (b) Box-plot (median and quartiles) showing the relation between the diameter and the degree of nodes.

described by Limpert et al. (2001); Kolmogorov–Smirnov test performed on $\log(S)$, $N = 210$, $Z = 1.21$, $p = 0.11$; Fig. 5b).

3.5. Diameter of the nodes

A previous study has shown that the node diameter is positively correlated to its degree (Buhl et al., 2004a). To analyse the diameter of the nodes, following the methods used in our previous study, vertex diameter was estimated by fitting a circle on the excavated space on the experimental picture, all the nodes forming dead-ends being excluded (peripheral and front nodes). The distribution of node diameter D in each experiment appeared to be log-normal (Kolmogorov–Smirnov test for a Gaussian distribution performed on $\log(D)$, $p > 0.05$ in all experiments; Fig. 6a). The diameter $D_{(k)}$ of the nodes of node degree k was positively correlated with k ($r_s = 0.522$; $N = 558$; $p < 0.001$; Fig. 6b). The skewedness of the distribution of node diameters thus partly results from the fact that the node diameter increases with the node degree. At the simple T shaped intersections (node degree $k = 3$) the median node diameter was $D_{(3)} = 10.36$ mm, while it reached $D_{(8)} = 42.32$ mm for nodes having the largest node degree $k = 8$.

4. Model description

We developed a spatially explicit model entirely based on the preceding experimental quantification (Table 1), that is, all parameters were estimated only from the data for the disk sand patch. In our model, a simulated network was described as a graph in the same way as in the experiments. The time unit was set to 1 min and a simulation ended when the total network length had reached a value randomly chosen in the Gaussian distribution of total network length $L = 1723$ mm (± 533 SD) observed in the experiments. Our choice to stop simulations at a particular network length rather than time was motivated by previous work on the regulation of tunnelling activity: (1) It has been shown that *Messor sancta* ants regulate tunnelling activity with network size and stop digging at a well defined size that is proportional to the number of ants (Buhl et al., 2005); (2) Stopping runs with this network length criterion resulted in simulations of 58.3 h (± 29.6 SD) on average, which is a timescale consistent with our previous

Table 1
Model parameters and values. Mean ± SD are given when the parameter was used to generate a random number from a Gaussian distribution

Param	Value	Units	Description
L	1723 ± 533	mm	Total network length
G_{max}	18	—	Total number of peripheral germs
P_g	0.0011	min^{-1}	Probability to initiate a peripheral germ
P_l	5.26×10^{-6}	$mm^{-1}\,min^{-1}$	Probability to initiate a lateral germ
P_n	0.69	—	Probability for a lateral germ to appear on an edge
$\alpha \pm \sigma$	0 ± 8.44	degrees	Angle formed between the tunnel and the perpendicular to the periphery of the sand patch or the edge
D_3	10.36	mm	Initial node diameter
S^*	0.062	$mm\,min^{-1}$	Tunnel growth speed

observation that digging activity stops during the third day (Buhl et al., 2005).

4.1. Initiation of new tunnels

Similarly to the experiments, a tunnel initiation corresponds to a front node that moves with the tunnel extension. This node is connected to the node where the initiation took place by a new edge. We considered two types of tunnel initiations resulting from peripheral or lateral germs.

(i) Initiation of peripheral germs: at the beginning of a simulation, a number of G_{max} potential peripheral germs with diameter D_n are created at random positions on the periphery of the sand patch (but with no overlapping between nodes). Each peripheral germ can then start to grow at each time unit according to the probability P_g.

(ii) Initiation of lateral germs: At each time step, a lateral germ can be initiated randomly along the edges with a probability P_l per unit of time and network length. When a lateral germ is created, it has a probability P_n to emerge from an edge; otherwise it will emerge from a previously existing node.

- Initiation from an edge: the edge is selected among all edges with a probability that is proportional to its length. A new lateral node is then created at a random position along the selected edge.
- Initiation from an existing node: the node is selected at random among all existing nodes.

4.2. Tunnel progression

Both peripheral germs and lateral germs emerging from an edge start with an angle β with respect to the tangent to the periphery of the sand patch or the edge, respectively. This angle is generated from a Gaussian distribution characterized by a mean α and a standard deviation $\sigma.\alpha$ corresponds to the direction of the normal vector to the periphery of the sand patch (for a peripheral germ) or the perpendicular to the edge where initiation took place (for a lateral germ initiated on an edge). In the case of the lateral germs that emerge from an existing node, the orientation of the new tunnel front is fixed to a random angle β chosen in a uniform distribution $[0,2\Pi[$.

At each time step, all front nodes progress with a constant speed S^* and keep their orientation constant.

4.3. Rules of collision

The growth of a tunnel ends when it intersects with another element, namely another edge, node or the periphery of the sand patch (see appendix for details).

5. Comparison of the model predictions with the experimental results

To compare the model predictions with the experimental results, the simulations were run in a disk ($N = 5000$) and a square geometry ($N = 5000$) corresponding to those used in experiments.

5.1. Basic characteristics

Both experimental and simulated networks in disk and square environment could comprise several connected components (Fig. 7). However, the largest connected component always included the vast majority of vertices (over 80%, see Table 2), while the other connected components were most frequently isolated galleries (2 vertices and 1 edge or small trees), which were initiated from the periphery and never merged with other galleries.

A Kruskal–Wallis test showed a significant variation between groups (experiments and simulations in each sand patch geometry; see Table 2) for most of the basic characteristics, but post-hoc comparisons (T3 Dunnet test) revealed that for all measures excepted the number of connected components, the only significant differences occurred between the two simulation groups, i.e. the disk and square environment. The number of nodes (n), edges (m), faces (f) and mean node degree ($\langle k \rangle$) were all slightly higher in the square than in the disk simulation. A similar tendency appeared also in the experiments, but was non-significant maybe due to the lower number of replicates and the high variability of these measures. The number of connected components (n_C) was significantly lower in the simulations with the square sand patch than in the

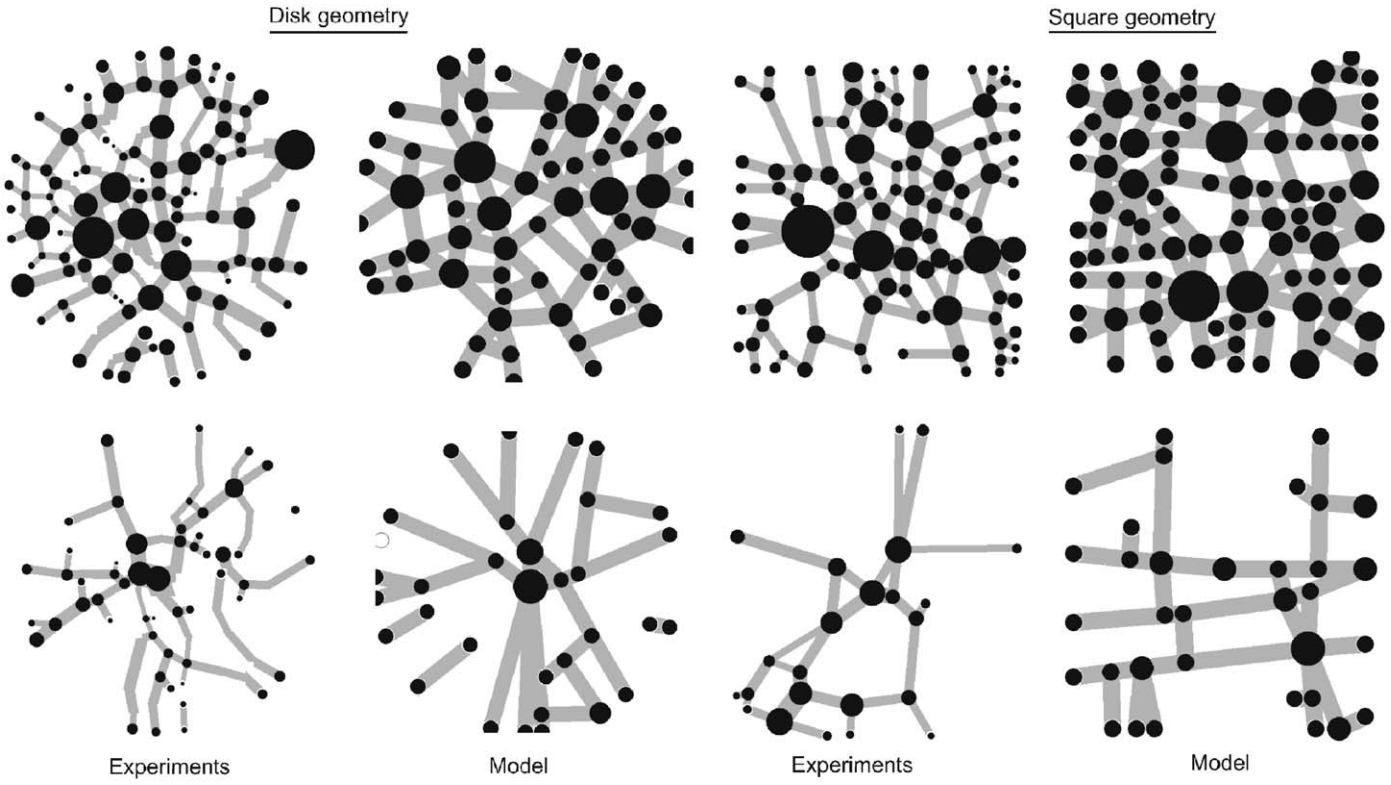

Fig. 7. Examples of networks obtained with a disk and a square sand patch geometry shown for the experiments and the model. The upper line shows examples of dense networks while the lower shows examples of sparse networks.

Table 2
Basic characteristics of the graphs obtained in experimental and simulated networks (n_C: number of connected components; V_l/V: relative size of the largest connected component, corresponding to the ratio between the number of nodes contained in the largest connected component and the total number of nodes in the network; n: number of nodes; m: number of edges; $\langle k \rangle$: mean node degree; f: number of faces; M: meshedness coefficient; ε: allometric exponent in the relation between the number of edges and the number of nodes; ξ: skewedness parameter in the exponential decay of the tail of the node degree distribution. Statistics corresponds to the Kruskal-Wallis test; $\pm$represents SD for all mean values, except for slope estimates ε and ξ where it represents SE

	n_C	V_l/V	n	m	$\langle k \rangle$	f	M	ε	ξ
Disk									
Exp.	3.95±0.56	0.83±0.11	51.2±22.0	63.5±31.3	2.40±0.26	13.4±10.3	0.122±0.06	1.16±0.037	0.98±0.04
Sim.	2.60±0.03	0.88±0.23	45.4±20.4	57.7±31.2	2.39±0.36	13.3±11.4	0.123±0.07	1.22±0.001	1.02±0.03
Square									
Exp.	1.67±0.8	0.87±0.15	71.8±29.3	89.9±40.7	2.45±0.19	19.11±12.2	0.127±0.04	1.10±0.041	0.73±0.09
Sim.	1.84±0.03	0.89±0.21	49.3±21.2	62.59±32.4	2.41±0.33	14.2±11.8	0.123±0.07	1.21±0.001	0.85±0.02
χ^2	891.8	35.3	38.7	11.2	25.2	17.1	0.115	—	—
p	<0.001	<0.001	<0.001	0.011	<0.001	0.001	0.99	—	—

simulations and experiments with the disk sand patch. There was a similar but non-significant trend for the experiments with the square sand patch to have a lower number of connected components than in the disk sand patch geometry.

5.2. Allometric relation between edges and nodes

Though the mean size of the network exhibited variability and changed between disk and square simulation, the increase of the number of edges with the number of nodes was well characterized by an invariant allometric law with an exponent ε significantly higher than 1 in all groups (Table 2; the test against slope $\varepsilon = 1$ gave $p < 0.05$ for all groups). In each sand patch geometry, disk or square, the model reproduced very well this characteristic of experimental networks (Fig. 8). Given the Euler formula, the rate at which the number of edges increases with the number of nodes has direct consequences on the formation of faces and the degree of meshedness in

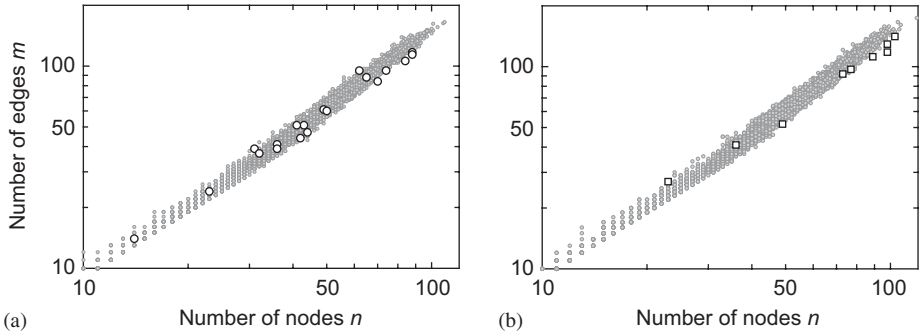

Fig. 8. Allometric relation between the number of edges m and the number of nodes n shown by the log-log representation of the data in the disk (a) and the square geometry (b). Both in experiments (open symbols) and simulations (grey closed symbols), the relation between m and n is a power law with an exponent value higher than 1 (see text and Table 2).

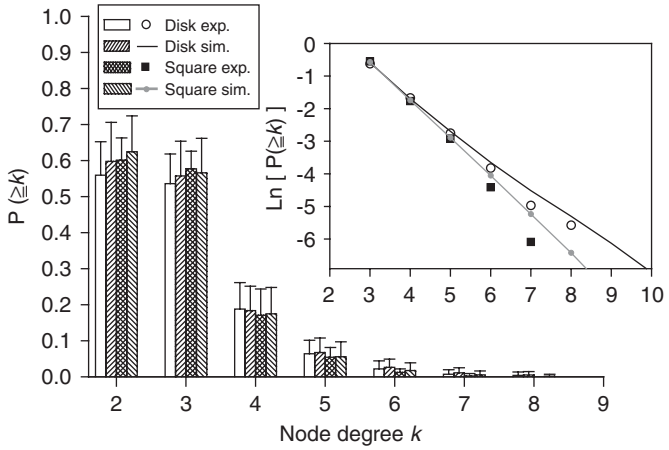

Fig. 9. Cumulative distribution of the node degrees k (mean $\pm$ SD) for the disk and the square geometry in experiments and simulations. The semi-logarithmic representation of the distributions (inset) reveals an exponential decay of the distribution tails.

networks. Whatever the group, the meshedness coefficient did not vary significantly and appeared to be a clear invariant of the network topology that the model did reproduce accurately (Table 2).

5.3. *Effect of the sand patch geometry on the node degree distributions*

In both the experiments and the model, the node degree distributions had a similar shape whatever the geometry of the sand patch (Fig. 9). The distribution tails were short and were well approximated by an exponential decay of the form $P(k) \sim e^{-k/\xi}$, where ξ is a constant that represents the skewedness of the tail. In the disk, the model reproduced particularly well the distribution tail observed in the experiments, with very close values for the ξ parameter. The effect of the sand patch geometry appeared similar in experiments and simulations: the skewedness (ξ) of the distribution tail is slightly lower in the square than in the disk geometry. This effect may be due to the fact that the disk geometry favours the convergence of the peripheral germs to the centre of the disk, which may lead to a more frequent collision between tunnels on the same nodes.

6. Discussion

In this work, we have characterized the growth dynamics of tunnelling networks dug by groups of ants. In the experiments with a disk sand patch, we have shown that the initiation of new tunnels can be described by two constant probabilities, whether the tunnels were initiated on the periphery or during branching events inside the sand patch. This statistical quantification of the network growth events allowed us to build a model of tunnel growth based on a few parameters and this model was able to reproduce the main topological characteristics of the networks that we observed in our experiments. In particular, we have shown that several topological invariants observed in the experiments, such as the allometric relation between edges and nodes, the degree of meshedness and the shape of the node degree distribution can emerge from a simple process of tunnel growth in a finite space.

Our model was entirely based on rules that were statistically quantified in the standardized conditions of the disk geometry. We then studied the effect of changing the sand patch geometry from a disk to square of equivalent surface. In the model, this resulted in an invariance of the meshedness coefficient but also a trend for the node degree distribution to be slightly less skewed. This trend probably results from the fact that the disk sand patch tends to concentrate more tunnels toward the centre of the set-up than the square does, resulting in more frequent high node degrees in the former. Another effect of the sand patch geometry was a decrease in the number of connected components in the square sand patch in comparison with the disk sand patch; the origin of this effect remain an open question.

Experiments aiming at validating the model predictions yielded similar results. Further validations may consist in studying how the topological properties change when tunnels start to grow from a single initiation point at the centre of a sand patch and extend toward the periphery.

This would be a relevant issue regarding the morphogenesis of a nest in natural conditions since this mode of network expansion has been observed in the superficial part of the nest of the ant *Pogonomyrmex badius* (Tschinkel, 2004). The model could be easily extended to this situation by replacing the peripheral initiations by tunnels emerging directly from a single central node, while keeping the same rules of initiations for lateral branching.

The nests built by many ant species in natural conditions exhibit a particular vertical profile, called "top-heavy", that corresponds to an exponential decay of the density of nest elements with respect to depth (Mikheyev and Tschinkel, 2004; Tschinkel, 2003, 2004). This pattern might reflect changes in the composition of the soil with respect to depth, but the invariance of the relation whatever the nest size and maximal depth suggests that it results from other factors (Mikheyev and Tschinkel, 2004; Tschinkel, 2004). One of the predictions of the model, in particular its lateral branching rule, is that the oldest parts of a network should be the more branched. An application of our model in a geometry where an initial gallery starts from the surface and extends downward and vertically, which can then branch through lateral initiations, may thus reproduce a similar vertical density pattern as the one observed in natural nests.

Branching processes may account for several invariant properties in network structures such as subterranean ant nests. It may also help to understand inter-specific differences in nest structure. A next step will be to study the sensitivity of topological properties to the parameter values in our model and to determine whether it is possible to generate very different forms of networks when the same rules are used but their parameter values are changed. Moreover, we chose to focus our study on an intermediate level of observation, where tunnels represented the basic unit of modelling rather than individual ants; the link between the probabilities of tunnel initiations and the ants' individual behaviour and interactions remains to be studied. The model assumes initiations of tunnels that are independent of each other, as well as independent and equal activity at every front node, but this apparent independence is more likely to reflect the complex outcome of interactions among many individuals. For example, it has been suggested that interplay between recruitment processes, interactions between ants (such as overcrowding) and their densities at digging sites might have a critical role in the initiation of new tunnels and branching events (Rasse, 1999). Therefore, further detailed analysis of tunnelling behaviour will be required to determine what are the key factors in ant behaviour that influence tunnel initiation and growth.

There has been a large number of studies addressing graph growth by modelling events of recombination or "attachment" between nodes (Albert and Barabasi, 2002; Bollobas, 1985; Dorogovtsev and Mendes, 2003; Erdös and Rényi, 1959; Watts, 1999). In these models, nodes exist independently of edges. The network growth results mainly from the creation and removal of edges which do not represent constructed elements but rather interactions. These models have constituted a useful theoretical background to study the origin of the topology of several real world networks such as networks of social and molecular interactions, or some technological networks where nodes exist independently from edges. However, no model of graph growth has yet taken into account a widespread phenomenon observed in many natural networks: that the growth of elements that correspond to "edges" can contribute to the emergence of nodes by the occurrence of branching and fusing events. This is the case of tunnelling networks in the subterranean nests of many ants (Cassill et al., 2002; Mikheyev and Tschinkel, 2004; Tschinkel, 2003, 2004) and termites (Grassé, 1984), the foraging tunnel systems of many termites (Darlington, 1982; Grassé, 1984; Lys and Leuthold, 1991) and of some subterranean rodents, such as mole-rats (Davies and Jarvis, 1986; Jarvis and Sale, 1971; Le Comber et al., 2002). This is also the growth mode of some fungal networks (Boddy et al., 1999), leaf vascular networks (Couder et al., 2002) or crack patterns (Allain and Limat, 1995; Aström and Timonen, 1997).

Though there exist well established paradigms to study the branching pattern of pure tree-networks, namely the Horton–Strahler method (Horton, 1945; Strahler, 1957) and its variants (Dodds and Rothman, 2000a–c; Turcotte et al., 1998), these methods cannot be applied to networks where cycles[1] are formed. It has been suggested that the formation of cycles in branching patterns, frequently observed in biological networks, may have important functional properties. Indeed, it has been recently shown (Buhl et al., 2004b) that the meshedness of ant tunnelling networks is correlated with efficiency (in term of minimization of detours in the path system) and robustness (in terms of disconnections). Remarkably, the observed ant tunnelling networks correspond to a particular topological class characterized by a combination of low costs (in terms of network length) with high efficiency and robustness (Buhl et al., 2004b). The exploration of simple network growth models such as the one we have presented in this paper will allow determination of the parameter regions where such advantageous characteristics can be obtained. More generally, the methodology based on the use of embedded graphs to quantify network growth rules may be useful to study the topology and geometry of other networks where the structure results from the extension of branching and fusing elements.

Acknowledgements

We thank Vincent Fourcassié, Christian Jost and Iain Couzin for many helpful discussions and comments. We thank the anonymous referees for their helpful comments

[1]A path that starts from a node and ends at the same one without going twice through the same edge.

and suggestions. This research was supported by the "Programme Cognitique". J. Buhl was supported by a research grant from the French Ministry of Education, Research and Technology. J.L. Deneubourg is research associate of the Belgian National Foundation for Scientific Research.

Appendix. Rules of collision

Consider an active front i and any other node j of the graph. d_{ij} is the Euclidian distance between the centres of the nodes i and j. D_i and D_j are the diameters of the node i and j respectively.

(1) Collision between nodes: if $d_{ij} < (D_i/2) + (D_j/2)$, the node i has merged with the node j and is suppressed. The edge connected to i becomes connected to j. As a consequence of the merging of i on j, the new surface of the node j becomes $S_{j+i} = S_j + \pi(D_i/2)^2$ and its new diameter is thus $D_{j+i} = 2\sqrt{S_{j+1}/\pi}$.
(2) Collision with an edge: A front node collides with an edge if the Euclidian distance between the centre of node i and its orthogonal projection h on the edge is lower than D. The node i takes the position h and takes the *internal* type. The collided edge is segmented into two new edges connected to this new node and to one of the extremities of the previous edge.
(3) Collision with the periphery of the sand patch: if the front node i arrives at a position on the periphery of the sand patch, its growth is stopped. The node i becomes an *external* node with a diameter D.

Merging between stopped nodes

Two nodes merge if they overlap. Consider two nodes i and j with their respective diameter D_i and D_j and d_{ij} the Euclidian distance between their centres. If $d_{ij} < (D_i + 2)/(D_j + 2)$ and $D_i < D_j$, the node i has merged in the node j and is suppressed. All edges connected to i thus become connected to j.

References

Albert, R., Barabasi, A.L., 2002. Statistical mechanics of complex networks. Rev. Mod. Phys. 74, 47–97.
Allain, C., Limat, L., 1995. Regular patterns of cracks formed by directional drying of a colloidal supension. Phys. Rev. Lett. 74, 2981.
Aström, J., Timonen, J., 1997. Fragmentation by crack branching. Phys. Rev. Lett. 78, 3677.
Boddy, L., Wells, J.M., Culshaw, C., Donnelly, D.P., 1999. Fractal analysis in studies of mycelium in soil. Geoderma 88, 301–328.
Bollobas, B., 1985. Random graphs. Academic Press, London.
Brian, M.V., 1983. Social insects: Ecology and Behavioural Biology. Chapman & Hall, London.
Buhl, J., Deneubourg, J.L., Grimal, A., Theraulaz, G., 2005. Self-organized digging activity in ant colonies. Behav. Ecol. Sociobiol. 58, 9–17.
Buhl, J., Gautrais, J., Deneubourg, J.L., Theraulaz, G., 2004a. Nest excavation in ants: group size effects on the size and structure of tunneling networks. Naturwissenschaften 92, 602–606.
Buhl, J., Gautrais, J., Solé, R.V., Kuntz, P., Valverde, S., Deneubourg, J.L., Theraulaz, G., 2004b. Efficiency and robustness in ant networks of galleries. Eur. Phys. J. B 42, 123–129.
Cassill, D., Tschinkel, W.R., Vinson, S.B., 2002. Nest complexity, group size and brood rearing in the fire ant, *Solenopsis invicta*. Insectes Soc. 49, 158–163.
Cerdan, P., 1989. Etude de la biologie, de l'écologie et du comportement des fourmis moissonneuses du genre *Messor* (Hymenoptera, Formicidae) en Crau. Ph.D. Thesis, Université de Provence, Aix-Marseille I.
Couder, Y., Pauchard, L., Allain, C., Adda-Bedia, M., Douady, S., 2002. The leaf venation as formed in a tensorial field. Eur. Phys. J. B 28, 135–138.
Darlington, J.P.E.C., 1982. The underground passages and storage pits used in foraging by a nest of the termite *Macrotermes michaelseni* in Kadjiado, Kenya. J. Zool. Lond. 198, 237–247.
Davies, K.C., Jarvis, J.U.M., 1986. The burrrow systems and burrowing dynamics of the mole-rats *Bathyergus suillus* and *Cryptomis hottentus* in the fynbos of the south-western Cape, South Africa. J. Zool. Lond. 209, 125–147.
Délye, G., 1971. Observations sur le nid et le comportement constructeur de *Messor arenarius*. Insectes Soc. 18, 15–20.
Dodds, P.S., Rothman, D.H., 2000a. Geometry of river networks. I. Scaling, fluctuations, and deviations. Phys. Rev. E 63, 016115.
Dodds, P.S., Rothman, D.H., 2000b. Geometry of river networks. II. Distribution of component size and number. Phys. Rev. E 63, 016116.
Dodds, P.S., Rothman, D.H., 2000c. Geometry of river networks. III. Characterization of component connectivity. Phys. Rev. E 63, 016117.
Dorogovtsev, S.N., Mendes, J.F.F., 2003. Evolution of Networks—From Biological Nets to the Internet and WWW. Oxford University Press, Oxford.
Erdös, P., Rényi, A., 1959. On random graphs I. Publ. Math. Debrecen 5, 290–297.
Frisch, K.v., 1975. Animal architecture. Hutchinson, London.
Grassé, P.P., 1984. Termitologia, Tome II. Fondation des sociétés. Construction. Masson, Paris.
Horton, R.E., 1945. Erosional development of streams and their drainage basins; hydrophysical approach to quantitative morphology. Bull. Geol. Soc. Am. 56, 275–370.
Imamura, S., 1982. Social modifications of work efficiency in digging by the ant, *Formica yessensis* Forel. J. Fac. Sci. Hokkaido Univ. Ser. VI Zool. 23, 128–142.
Jarvis, J.U.M., Sale, J.B., 1971. Burrowing and burrow patterns of East African mole-rats *Tachyoryctes*, *Heliophobius* and *Heterocephalus*. Zool. Lond. 163, 451–479.
Le Comber, S.C., Spinks, A.C., Bennett, N.C., Jarvis, J.U.M., Faulkes, C.G., 2002. Fractal dimension of African mole-rat burrows. Can. J. Zool. 80, 436–441.
Limpert, E., Stahel, W.A., Abbt, M., 2001. Log-normal distributions across the sciences: Keys and clues. Bioscience 51, 341–352.
Lys, J.-A., Leuthold, R.H., 1991. Morphology of the gallery system around the nest and gallery development under experimental conditions in the termite *Macrotermes bellicosus* (Smeathman). Insectes Soc. 38, 63–76.
Mikheyev, A.S., Tschinkel, W.R., 2004. Nest architecture of the ant *Formica pallidefulva*: structure, costs and rules of excavation. Insectes Soc. 41, 30–36.
Nishizeki, T., Chiba, N., 1988. Planar Graphs. Theory and Algorithms, North-Holland, Amsterdam.
Rasse, P., 1999. Etude sur la régulation de la taille et sur la structuration du nid souterrain de la fourmi *Lasius niger*. Ph.D. Thesis, Université Libre de Bruxelles, Brussells.
Rasse, P., Deneubourg, J.L., 2001. Dynamics of nest excavation and nest size regulation of *Lasius Niger* (Hymenoptera: Formicidae). J. Insect Behav. 14, 433–449.

Solé, R.V., Ferrer i Cancho, R., Montoya, J.M., Valverde, S., 2002. Selection, tinkering and emergence in complex networks. Complexity 8, 20–33.

Strahler, A.N., 1957. Quantitative analysis of watershed geomorphology. Trans. Am. Geophys. Union 38, 913–920.

Sudd, J.H., 1969. The excavation of soil by ants. Z Tierpsyschol. 26, 257–276.

Sudd, J.H., 1970a. Specific patterns of excavation in isolated ants. Insectes Soc. 17, 253–260.

Sudd, J.H., 1970b. The response of isolated digging worker ants [*Formica lemani* and *Lasisus niger*] to tunnels. Insectes Soc. 17, 261–271.

Sudd, J.H., 1971. The effect of tunnel depth and of working in pairs on the speed of excavation in ants (*Formica lemani* Bondroit). Anim. Behav. 19, 677–686.

Sudd, J.H., 1975. A model of digging behaviour and tunnel production in ants. Insectes Soc. 22, 225–235.

Thomé, G., 1972. Le nid et le comportement de construction de la fourmi *Messor ebeninus*, Forel (Hymenoptera, Formicoïdea). Insectes Soc. 19, 95–103.

Tschinkel, W.R., 1987. Seasonal life history and nest architecture of a winter-active ant, *Prenolepis imparis*. Insectes Soc. 34, 143–164.

Tschinkel, W.R., 2003. Subterranean ant nests: trace fossils past and future? Palaeogeogr. Palaeoclimatol. Palaeoecol. 192, 321–333.

Tschinkel, W.R., 2004. The nest architecture of the Florida harvester ant, *Pogonomyrmex badius*. J. Insect. Sci. 4, 〈http://insectscience.org/4.21/〉.

Turcotte, D.L., Pelletier, J.D., Newman, W.I., 1998. Networks with side branching in biology. J. Theor. Biol. 193, 577–592.

Watts, D.J., 1999. Small Worlds: The Dynamics of Networks Between Order and Randomness. Princeton University Press, Princeton.

Zar, J.H., 1999. Biostatistical Analysis, 4th ed. Prentice-Hall, Upper Saddle River, NJ.